General Relativistic Simulations of the Quasicircular Inspiral and Merger of Charged Black Holes: GW150914 and Fundamental Physics Implications

Gabriele Bozzola[1,*] and Vasileios Paschalidis[2,†]
[1]*Department of Astronomy, University of Arizona, Tucson, Arizona 85721, USA*
[2]*Departments of Astronomy and Physics, University of Arizona, Tucson, Arizona 85721, USA*

(Received 1 July 2020; revised 2 October 2020; accepted 5 January 2021; published 26 January 2021)

We perform general-relativistic simulations of charged black holes targeting GW150914. We show that the inspiral is most efficient for detecting black hole charge through gravitational waves and that GW150914 is compatible with having charge-to-mass ratio as high as 0.3. Our work applies to electric and magnetic charge and to theories with black holes endowed with U(1) (hidden or dark) charges. Using our results, we place an upper bound on the deviation from general relativity in the dynamical strong-filed regime of Moffat's modified gravity.

DOI: 10.1103/PhysRevLett.126.041103

Introduction.—According to the "no-hair" conjecture [1–6], general-relativistic black holes are described by four parameters: mass, angular momentum, and electric and magnetic charge. It is assumed, often implicitly, that astrophysical black holes have negligible charge because of the expectation that they would quickly discharge due to the interaction with a highly conducting gaseous environment or by the spontaneous production of electron-positron pairs [7–12]. However, observational data unequivocally supporting this expectation are currently absent, and any existing constraints on black hole charge depend crucially on the assumptions of the models employed (e.g., [13,14]). Gravitational-wave observations offer a model-independent path to constraining the charge of astrophysical black holes. The electromagnetic fields influence the spacetime, altering the gravitational-wave emission compared to an uncharged binary. These deviations are accurately modeled in Einstein-Maxwell theory and are potentially detectable by Laser Interferometer Gravitational-Wave Observatory (LIGO)-Virgo and future gravitational-wave observatories. As we will discuss below, the word "charge" here is an umbrella term that includes, among other things, electric or magnetic charge, dark charge, or gravitational charge due to modifications to general relativity.

In this Letter, we initiate a robust program for constraining black hole charge by combining LIGO-Virgo observations with novel numerical relativity simulations. Our focus here is on event GW150914 [15]. (The possibility that GW150914 involved charged black holes has been invoked [16–18] to explain the observation of a coincident electromagnetic signal by the Fermi-gamma-ray-burst monitor [19,20]. This association is debated as others satellites did not detect the event [21–24].) Using the event's sky location and the calibrated LIGO noise, we compute the "mismatch" (defined later) between the uncharged case and various charged ones. The observed signal-to-noise ratio sets a threshold mismatch above which two waveforms are distinguishable [25–28]. Hence, assuming that the observed waveform is described by uncharged, nonspinning black holes, we find the minimum charge that would be detectable by LIGO.

For uncharged binaries, when black hole spin is neglected and the mass ratio is fixed, knowing one "mass" parameter determines the entire gravitational waveform. We will use here the "chirp mass" $\mathcal{M}$ [29]. In the case of inspirals of charged binaries, this parameter can be degenerate with the charge itself [30–33]. This can be understood as follows: In Newtonian physics, gravity and electromagnetism are both central potentials, so the electrostatic force can be accounted for by introducing an effective Newton constant $\tilde{G}$. Consider two bodies with mass m_1, m_2 and charge $q_1 = \lambda_1 m_1$, $q_2 = \lambda_2 m_2$ (λ being the charge-to-mass ratio); the dynamics of the system is indistinguishable from one with uncharged bodies with gravitational constant $\tilde{G} = (1 - \lambda_1\lambda_2)G$. Since the relationship between chirp mass and gravitational-wave frequency evolution involves Newton's constant, introducing charges corresponds to rescaling the chirp mass while keeping G fixed. This degeneracy is broken by electromagnetic radiation reaction and the field self-gravity.

Adopting the effective Newton constant approach, previous studies [30–35] constructed Newtonian-based waveforms by considering the Keplerian motion of two charged bodies and accounting for loss of energy via quadrupolar emission of gravitational waves and dipolar emission of electromagnetic ones. The authors of [31] computed the bias in the binary parameters due to the charge-chirp mass degeneracy. With similar tools, Wang *et al.* [35] performed a full Bayesian analysis with Gaussian noise to place preliminary constraints on charge using events in the first gravitational-wave transient catalog [36]. Alternatively, the dipole can be constrained directly by adding a -1

post-Newtonian (PN) term to describe the loss of energy due to dipole emission [35], as first done for modified theories of gravity [37]. In [37,38], it was found that the dipole can be constrained more effectively in the inspiral (also noted in [30,33] with explicit reference to charges). One of the main limitations of these (post-)Newtonian methods is that they strictly apply only to the early inspiral. However, binaries like GW150914 are in the regime where numerical relativity simulations are necessary for accurate modeling [15]. Therefore, existing constraints on black hole charge in events where only a few orbits to merger have been detected are at best preliminary. Moreover, the effective Newton constant approach does not capture the physics in cases when only one of the two components is charged, and when the dipole moment vanishes, these previous approaches do not treat quadrupole electromagnetic emission. This is very important because, as we demonstrate here, it is binaries with near vanishing dipole moment that place the weakest constraint on black hole charge.

A second avenue for constraining black hole charge is through the ringdown signal. In the context of mergers of charged black holes, this was first studied in [30,33] in the limit of small charge, using the method of geodesic correspondence. Via a Fisher matrix analysis, it was noticed that the ability to constrain charge depends strongly on the signal-to-noise ratio, so GW150914 cannot be used to place strong bounds on the charge-to-mass ratio λ of the final black hole. However, as the authors remarked, these results should be considered only as qualitative, since higher-order terms in λ were neglected.

Instead of using approximations, here we solve the full nonlinear Einstein-Maxwell equations, extracting accurate gravitational waves to overcome the shortcomings of previous approaches. We perform numerical-relativity simulations of black holes with (1) same charge-to-mass ratio (which we will indicate with λ_+^+), (2) same charge-to-mass ratio but opposite sign (λ_-^+), and (3) only one charged black hole (λ_0^+). Einstein-Maxwell theory has no intrinsic scale, so our simulations scale with the total Arnowitt-Deser-Misner (ADM) mass of the system M [39]. Thus, we can explore arbitrary chirp masses with each simulation. We compute the mismatch between gravitational waveforms generated by charged and uncharged binaries with a range of different masses to account for the degeneracy: black hole charge is constrained when the mismatch is larger than a value set by the signal-to-noise ratio [25–28] for all possible values of the chirp mass.

An important advantage of our approach is that it furnishes a first-principles calculation based on fundamental theories and does not rely on particular models. As a result, the mathematical formulation we employ has direct fundamental physics applications. Examples are dark matter theories (e.g., dark electromagnetism, hidden sector [31,40–45], or minicharged particles [30,46–53]). These theories allow black holes to be highly charged, since neutralization arguments do not apply. Moreover, with a duality transformation [54], our work also constrains black hole magnetic charge (e.g., from primordial magnetic monopoles [55,56]). Our simulations are also useful for the generation and calibration of gravitational-wave template banks that target these systems.

Furthermore, our research targets theories of gravitation where gravity is also mediated by a vector field, like the scalar-tensor-vector gravity developed in [57] to explain "dark matter" phenomenology without dark matter. This theory [also known as Modified Gravity (MOG)], has been widely studied in the past and can pass several tests, such as Solar System ones [58] (see also [57,59–67]; for a summary of the formulation, assumptions, and successes of the theory, see [62]). MOG features a scalar field that makes gravity stronger by increasing Newton's constant and a Proca field that counteracts this effect in the short range. When considering systems much smaller than the galactic scale, the vector field can be considered massless and the scalar field becomes constant and modifies Newton's constant to $G_{\mathrm{eff}} = G(1+\alpha)$. According to MOG, a body with mass M has a gravitational charge Q that is associated with the vector field and is proportional to M. "Moffat's prescription" sets the constant of proportionality to $\sqrt{\alpha G_{\mathrm{eff}}/(1+\alpha)}$ so that the theory satisfies the weak equivalence principle [68]. In this limit, MOG differs mathematically from Einstein-Maxwell theory only in using G_{eff} instead of G, and when $\alpha = 0$ the theory becomes general relativity. This rescaling gives rise to the same degeneracy in the chirp mass and $\tilde{G}$ that we discussed above in the case of electromagnetism: in geometrized units, MOG solutions with mass M_{MOG} and gravitational constant $G_{\mathrm{eff}} = 1$ are equivalent to Einstein-Maxwell solutions with mass $M = M_{\mathrm{MOG}}(1+\alpha)$ and $G = 1$. Hence, by scanning through all possible values of the mass, a constraint on the charge-to-mass ratio translates in this theory to a constraint on $Q/M = \sqrt{\alpha/(1+\alpha)}$.

The results of this work depend on three basic assumptions: 1) Einstein-Maxwell theory is the correct description of charged black holes at the energy, length, and timescales we are investigating; 2) GW150914 is accurately modeled by waveforms from uncharged, nonspinning binary black holes with mass ratio 29/36—the value inferred for GW150914 [15]; and 3) the black hole spin and binary mass ratio remain that of GW150914 even in the case of nonzero charge. Spin and mass ratio may be degenerate with the charge, so the results presented in this Letter can be interpreted in two ways: if assumption 3 holds for GW150914, then our charge limits are *upper* bounds on the charge-to-mass ratio of the binary components, otherwise, they are lower bounds on the charge-to-mass ratio needed to leave detectable imprints in GW150914-like events. We will explore the effects of spin and mass ratio in future works. To further reduce the parameter space, we only consider black holes with the same charge-to-mass ratio bracketing the possibilities. This choice also ensures the applicability of our results to modified theories of gravity where the charge-to-mass ratio represents a coupling constant (as in MOG), in which case only systems with the same charge-to-mass ratio are relevant (in the limit we discussed above).

Methods.—We employ the EINSTEIN TOOLKIT [69–71] to solve the coupled Einstein-Maxwell equations in the $3+1$ decomposition of four-dimensional spacetime [39,72–75]. We report the general features of our approach here and leave the details for the Supplemental Material [76].

We performed simulations with charge-to-mass ratio $\lambda \in \{0.01, 0.05, 0.1, 0.2, 0.3\}$ with like or opposite charge for the two black holes (cases that we will designate as λ_+^+ and λ_-^+, where the superscript and subscript indicate the sign of the charge of the primary and the secondary, respectively) and only one charged black hole (λ_0^+). These cases are supplemented by an uncharged one (λ_0^0), a convergence study, and by simulations with $\lambda_+^+ = 0.4$, $\lambda_0^+ = 0.35$, and $\lambda_+^0 = 0.35$.

Full nonlinear evolutions of Einstein-Maxwell systems have already been performed in the past for head-on collisions of charged black holes [77,78]. Simulations of quasicircular inspirals are a nontrivial extension of that, as the generation of valid initial data with the solution of the constraint equations [74] is required. In [79] we presented TwoChargedPunctures, which solves this problem by adopting an extended Bowen-York formalism [80–82] and allows the generation of arbitrary configurations of charged black holes. We fix the initial coordinate separation to $12.1M$ and we choose the black hole initial linear momenta to yield a quasicircular inspiral using a 2.5 PN estimate after rescaling G to $\tilde{G}$.

We evolve the spacetime and electromagnetic fields with the open-source and well-tested LEAN and ProcaEvolve codes [83–86]. LEAN implements the Baumgarte-Shapiro-Shibata-Nakamura formulation of Einstein's equation [87,88], whereas ProcaEvolve evolves the electromagnetic vector potential with a constraint-damping scheme for the Gauss constraint. The evolution is on Cartesian CARPET [89] grids where the highest resolution is approximately $M/65$, with M being the binary ADM mass [39]. We extract gravitational waves based on the Newman-Penrose formalism [86,90], adopting the fixed-frequency integration method [91]. We decompose the signal into -2 spin weighted spherical harmonics and focus on the dominant $l=2$, $m=2$ gravitational-wave mode.

Two waveforms are considered experimentally indistinguishable if their mismatch is smaller than $1/(2\rho^2)$ [25–28], with ρ being the signal-to-noise ratio. For GW150914, $\rho = 25.1$ [92], so the threshold mismatch above which two signals are distinguishable is approximately 8×10^{-4}. We calculate the mismatch between strains h_1 and h_2 as $1 - \max \mathcal{O}(h_1, h_2)$, where $\mathcal{O}(h_1, h_2)$ is the overlap between the two signals (see Supplemental Material [76]), and the maximum is evaluated with respect to time shifts, orbital-phase shifts, and polarization angles [28,93]. The overlap calculation is performed in the frequency domain. We consider LIGO's noise curve at the time of GW150914 detection and adopt the GW150914 inferred sky location. For the uncharged signal, we set a source frame ADM mass $M = 65\ M_\odot$, and a luminosity distance of 410 Mpc, corresponding to cosmological redshift of ≈ 0.09 [94]. In the Supplemental Material [76], we discuss how different choices for these parameters affect the results. To account for the charge-chirp mass degeneracy, we compute the mismatch between gravitational waves from uncharged black holes and the ones from charged systems with different chirp masses $\mathcal{M}$. To vary the chirp mass, we rescale M by a factor that we indicate with $\mathcal{M}/\mathcal{M}_{00}$, where $\mathcal{M}_{00}$ is the chirp mass of the uncharged simulation. We estimate the error on the mismatch by comparing simulations at different resolutions.

Results and discussion.—The mismatch between a charged and the uncharged binary grows with the charge-to-mass ratio λ. So, we may place an upper bound on the charge by finding the value of λ at which the minimum mismatch (as we vary the chirp mass) is larger than 8×10^{-4}. We find that, assuming negligible spin and mass ratio of $29/36$, GW150914 constrains λ to be smaller than

$$\lambda_+^+ = 0.4, \qquad \lambda_-^+ = 0.2, \quad \text{and} \quad \lambda_0^+ = 0.35. \qquad (1)$$

Regardless of the value of the spin and the mass ratio, Eq. (1) provide lower bounds on λ needed to have detectable effects in GW150914-like events.

In our simulations, we always endow the more massive black hole with positive charge. Since the mass asymmetry of the system is small, we expect our conclusions to remain the same in the opposite case. The simulation with $\lambda_+^0 = 0.35$ confirms this expectation: the computed minimum mismatch differs by 10% from the $\lambda_0^+ = 0.35$ case. Thus, the effect of the mass asymmetry is small.

In Fig. 1, we show the mismatch between the uncharged simulation and charged ones as a function of the rescaling factor $\mathcal{M}/\mathcal{M}_{00}$ for the chirp mass. The figure has three sets of curves. Solid curves represent the mismatch computed on the entirety of the signal (i.e., all frequencies are included). In the top panels, these curves have minima below the threshold mismatch (horizontal solid line) for some value of $\mathcal{M}/\mathcal{M}_{00}|_{\min}$. Thus, gravitational waves from these charged configurations are indistinguishable from the signal that we adopt as true for GW150914. The opposite holds in the bottom panels. Therefore, under the assumptions of our study, GW150914 is compatible with involving charged black holes with Q/M up to about 0.3. The noise curve adopted plays an important role: if instead of the

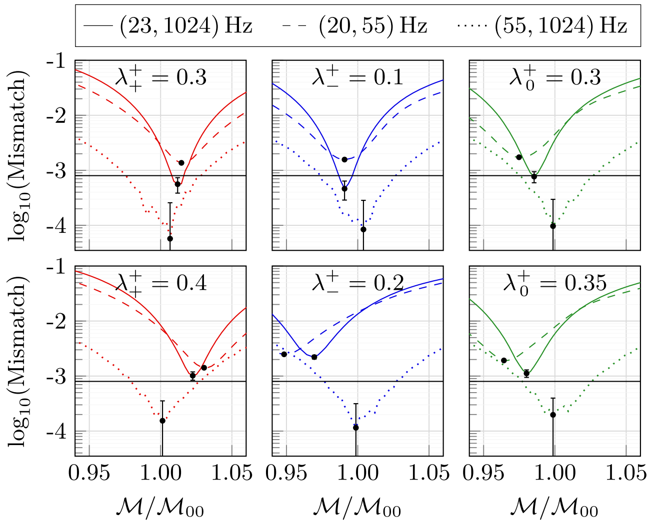

FIG. 1. Mismatch between the strains from uncharged black holes and from charged ones with chirp mass rescaled by $\mathcal{M}/\mathcal{M}_{00}$. Solid curves are the mismatch including all available frequencies (the entire signal), dashed ones are only restricting to the frequency range (23,55) Hz (inspiral) and dotted ones have frequencies restricted to (55,1024) Hz (merger and ringdown). The solid horizontal line is the detection threshold for GW150914 (8×10^{-4}). The top (bottom) row is the largest (smallest) value of λ (in our survey) compatible (incompatible) with GW150914. Red curves (left column) are for the simulation with $\lambda_+^+ = 0.3$ (top) and $\lambda_+^+ = 0.4$ (bottom), blue (central column) for $\lambda_-^+ = 0.1$ and $\lambda_-^+ = 0.2$, and green (middle column) for $\lambda_0^+ = 0.3$ and $\lambda_0^+ = 0.35$. The error bars shown are estimated comparing the standard resolution simulation with the one at higher resolution. We report the error bar only at minimum mismatch, but each point along the curve has the same level of error.

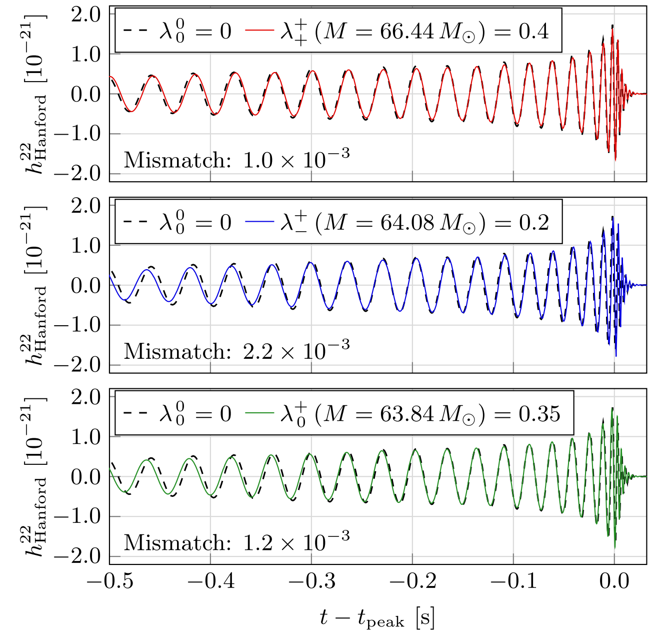

FIG. 2. Comparison between the (2,2) mode of the detector-response strain for Hanford for the simulations with no charges (dashed curves) and the ones with it, but with chirp mass $\mathcal{M}$ rescaled with respect to $\mathcal{M}_{00} = 28.095\,M_\odot$. Time and phase shifts are applied to minimize the mismatch between the two signals. All of these waveforms have two-detectors mismatch larger than the detection threshold for GW150914 of 8×10^{-4}, mostly coming from the inspiral phase.

realistic one, we consider the zero-detuned-high-power noise curve [95], the mismatch increases by a factor of about 3, making the top panels in Fig. 1 incompatible with the observation and, hence, distinguishable. Thus, it is important to use the realistic noise in these calculations.

Figure 1 reports two additional sets of curves: dashed lines, representing the mismatch computed including frequencies below 55 Hz and dotted ones for frequencies above 55 Hz. In other words, the dashed and dotted curves are the mismatch that would be computed if we had detected *only* the inspiral or *only* the plunge and merger phases. The frequency of 55 Hz marks conventionally the end of the *inspiral* phase [96]. Including a larger range of frequencies decreases the minimum mismatch (from dashed lines to solid). Hence, previous studies focusing only on the inspiral overestimate the mismatch and the bias in the extracted chirp mass.

Figure 1 shows that the mismatch is significantly higher in the inspiral, suggesting that it is the dominant contribution in the overall mismatch. Figure 2 further emphasizes this conclusion: we plot the strain the Hanford detector would observe, if there was no noise, i.e., $h^{22}_{\rm Hanford} = F_\times h^{22}_\times + F_+ h^{22}_+$, where F is the detector antenna pattern [92]. The dashed curves represent GW150914 and the solid ones are the strains from the charged simulations, rescaled and shifted to maximize the overlap. The plot shows that the greatest difference between charged and uncharged black holes arises in the earlier inspiral. Thus, signals that stay for a longer duration in LIGO-Virgo bands allow for stronger constraints on the charge. All waveforms in Fig. 2 have mismatch with GW150914 larger than 8×10^{-4}; hence the corresponding charge configurations are incompatible with GW150914.

One of the reasons why the merger + ringdown phase of the signal is not as informative as the inspiral is that the properties of the final black holes do not depend strongly on the initial charge configuration. In all our simulations, the mass of the final black hole is the same to within 1% ($M_{\rm final} \approx 0.96M$), and the dimensionless spin differs by at most 6% ($a_{\rm final}/M_{\rm final} \approx 0.66$). In particular, in our opposite charge cases, the final mass and spin have subpercent differences with respect to the uncharged case, and, as expected from relativistic estimates, the case with same charge has a lower spin [97]. This result agrees with [30,33]: a large charge or a large signal-to-noise ratio is required to extract the charge information from the ringdown.

Our full nonlinear study supports previous results that were obtained with parametrized methods. Constraints on the dipolar gravitational-wave emission were placed in [37,38] using Fisher matrix analysis based on phenomenological waveform models. Translated into an upper bound on the normalized electric dipole, the constraint becomes $\zeta = \lambda_1 - \lambda_2/\sqrt{1-\lambda_1\lambda_2} \lesssim 0.31$ [30,35]. Our work shows that $\zeta < 0.3$ (from the case with $\lambda_0^+ = 0.3$). However, our work goes further by placing a constraint on the individual black hole charge.

Our results can also be applied to the so-called theory of MOG [98]. At scales relevant for compact binary mergers, this theory replaces Newton's constant $G \to G_{\rm eff}$ and postulates the existence of a gravitational charge $Q = \sqrt{\alpha G_{\rm eff}/(1+\alpha)}M$. The difference in Newton's constant is degenerate with a change in chirp mass, which we thoroughly explored. Figure 1 shows that, when $\lambda_+^+ = 0.4$, no matter how the chirp mass is changed, it is not possible to reconcile GW150914 with the merger of charged black holes with $\lambda_+^+ = 0.4$. Hence, our study directly constrains $\alpha \lesssim 0.19$. This implies that the theory cannot deviate much from general relativity in the strong field, under the assumptions made in this Letter.

Conclusions.—In this Letter, we presented fully self-consistent general-relativistic simulations of the inspiral and merger of charged nonspinning black holes with mass ratio 29/36. We considered cases where both black holes are charged with the same charge-to-mass ratio (λ_+^+), opposite charge-to-mass ratio (λ_-^+), and only one black hole charged (λ_0^+). By comparing waveforms from uncharged systems to those from charged ones, we addressed the charge-chirp mass degeneracy and found that, assuming nonspinning black holes with mass ratio of 29/36 for GW150914, λ has to be smaller than

$$\lambda_+^+ = 0.4, \qquad \lambda_-^+ = 0.2, \quad \text{and} \quad \lambda_0^+ = 0.35. \tag{2}$$

These results hold under the assumption that spin and mass ratio play a secondary role. Independently of that, Eq. (2) provides a lower bound on the charge-to-mass ratio needed to leave measurable effects on the gravitational waves from GW150914-like events.

We found that the inspiral is the most constraining part of the signal for charge (Figs. 1 and 2). So, low-mass binaries, having more orbits in LIGO-Virgo bands, will likely yield tighter bounds on black hole charge. Our full nonlinear analysis confirms that it is challenging to constrain charge from the ringdown phase of merging charged black holes [30,33].

The bounds found in this study do not apply only to electric charge, but they can be directly translated to constraints on modified theories of gravity and exotic astrophysical scenarios, e.g., dark matter models [30], or primordial magnetic monopoles [55]. In this Letter, we applied our findings to Moffat's scalar-vector-tensor gravity (or MOG) [57] and constrained its α parameter to $\alpha \lesssim 0.19$ (note that $\alpha = 0$ is general relativity). Here, we did not consider the effects of black hole spin and the binary mass ratio, and including these parameters can introduce degeneracies that make the constraint less stringent. Applications to lower-mass black hole binary detections may be able to constrain this theory significantly in the strong-field dynamical regime.

In the future, we will consider systems with spinning black holes, different mass ratios, and asymmetric charge-to-mass ratio. With a large enough bank of simulations, we will produce surrogate models (e.g., [99]) to perform full parameter estimation of GW150914 and other LIGO-Virgo events.

We thank M. Zilhão for help on PROCAEVOLVE, J. R. Westernacher-Schneider for useful discussions, and D. Brown, V. Cardoso, J. Moffat, and U. Sperhake for comments on the Letter. We also wish to thank D. Brown for discussions on gravitational-wave data analysis. We are grateful to the developers and maintainers of the open-source codes that we used: their work was essential to the research presented here. This work was in part supported by NSF Grant No. PHY-1912619 to the University of Arizona. We acknowledge the hospitality of the Kavli Institute for Theoretical Physics (KITP), where part of the work was conducted. K. I. T. P. is partially supported by the NSF Grant No. PHY-1748958. Computational resources were provided by the Extreme Science and Engineering Discovery Environment (XSEDE) under Grant No. TG-PHY190020. X. S. E. D. E. is supported by the NSF Grant No. ACI-1548562. Simulations were performed on Comet and Stampede2, which is funded by the NSF through Grant No. ACI-1540931.

*gabrielebozzola@arizona.edu
†vpaschal@arizona.edu

[1] W. Israel, Event horizons in static vacuum space-times, Phys. Rev. **164**, 1776 (1967).
[2] B. Carter, Axisymmetric Black Hole Has Only Two Degrees of Freedom, Phys. Rev. Lett. **26**, 331 (1971).
[3] D. C. Robinson, Classification of black holes with electromagnetic fields, Phys. Rev. D **10**, 458 (1974).
[4] S. W. Hawking, Black holes in general relativity, Commun. Math. Phys. **25**, 152 (1972).
[5] R. Hansen, Multipole moments of stationary space-times, J. Math. Phys. (N.Y.) **15**, 46 (1974).
[6] P. T. Chruściel, J. L. Costa, and M. Heusler, Stationary black holes: Uniqueness and beyond, Living Rev. Relativity **15**, 7 (2012).
[7] R. M. Wald, Black hole in a uniform magnetic field, Phys. Rev. D **10**, 1680 (1974).
[8] G. W. Gibbons, Vacuum polarization and the spontaneous loss of charge by black holes, Commun. Math. Phys. **44**, 245 (1975).
[9] D. M. Eardley and W. H. Press, Astrophysical processes near black holes, Annu. Rev. Astron. Astrophys. **13**, 381 (1975).

[10] R. S. Hanni, Limits on the charge of a collapsed object, Phys. Rev. D **25**, 2509 (1982).

[11] Y. Gong, Z. Cao, H. Gao, and B. Zhang, On neutralization of charged black holes, Mon. Not. R. Astron. Soc. **488**, 2722 (2019).

[12] Z. Pan and H. Yang, Black hole discharge: Very-high-energy gamma rays from black hole-neutron star mergers, Phys. Rev. D **100**, 043025 (2019).

[13] L. Iorio, Constraining the electric charges of some astronomical bodies in Reissner-Nordström spacetimes and generic r^{-2}-type power-law potentials from orbital motions, Gen. Relativ. Gravit. **44**, 1753 (2012).

[14] M. Zajaček, A. Tursunov, A. Eckart, and S. Britzen, On the charge of the Galactic centre black hole, Mon. Not. R. Astron. Soc. **480**, 4408 (2018).

[15] B. P. Abbott *et al.* (LIGO Scientific and Virgo Collaborations), Observation of Gravitational Waves from a Binary Black Hole Merger, Phys. Rev. Lett. **116**, 061102 (2016).

[16] B. Zhang, Mergers of charged black holes: Gravitational-wave events, short gamma-ray bursts, and fast radio bursts, Astrophys. J. Lett. **827**, L31 (2016).

[17] S. L. Liebling and C. Palenzuela, Electromagnetic luminosity of the coalescence of charged black hole binaries, Phys. Rev. D **94**, 064046 (2016).

[18] F. Fraschetti, Possible role of magnetic reconnection in the electromagnetic counterpart of binary black hole merger, J. Cosmol. Astropart. Phys. 4 (2018) 054.

[19] V. Connaughton *et al.*, Fermi GBM observations of LIGO gravitational-wave event GW150914, Astrophys. J. Lett. **826**, L6 (2016).

[20] V. Connaughton *et al.*, On the interpretation of the Fermi-GBM transient observed in coincidence with LIGO gravitational-wave event GW150914, Astrophys. J. Lett. **853**, L9 (2018).

[21] B. P. Abbott, R. Abbott, T. D. Abbott, M. R. Abernathy, F. Acernese, K. Ackley, C. Adams, T. Adams, P. Addesso, R. X. Adhikari *et al.*, Localization and broadband follow-up of the gravitational-wave transient GW150914, Astrophys. J. Lett. **826**, L13 (2016).

[22] K. Hurley, D. S. Svinkin, R. L. Aptekar, S. V. Golenetskii, D. D. Frederiks, W. Boynton, I. G. Mitrofanov, D. V. Golovin, A. S. Kozyrev, M. L. Litvak, A. B. Sanin, A. Rau, A. von Kienlin, X. Zhang, V. Connaughton, C. Meegan, T. Cline, and N. Gehrels, The interplanetary network response to LIGO GW150914, Astrophys. J. Lett. **829**, L12 (2016).

[23] P. A. Evans *et al.*, Swift follow-up of the gravitational wave source GW150914, Mon. Not. R. Astron. Soc. **460**, L40 (2016).

[24] V. Savchenko, C. Ferrigno, S. Mereghetti, L. Natalucci, A. Bazzano, E. Bozzo, S. Brandt, T. J.-L. Courvoisier, R. Diehl, L. Hanlon, A. von Kienlin, E. Kuulkers, P. Laurent, F. Lebrun, J. P. Roques, P. Ubertini, and G. Weidenspointner, INTEGRAL upper limits on gamma-ray emission associated with the gravitational wave event GW150914, Astrophys. J. Lett. **820**, L36 (2016).

[25] É. É. Flanagan and S. A. Hughes, Measuring gravitational waves from binary black hole coalescences. II. The waves' information and its extraction, with and without templates, Phys. Rev. D **57**, 4566 (1998).

[26] L. Lindblom, B. J. Owen, and D. A. Brown, Model waveform accuracy standards for gravitational wave data analysis, Phys. Rev. D **78**, 124020 (2008).

[27] S. T. McWilliams, B. J. Kelly, and J. G. Baker, Observing mergers of nonspinning black-hole binaries, Phys. Rev. D **82**, 024014 (2010).

[28] B. P. Abbott, R. Abbott, T. D. Abbott, M. R. Abernathy, F. Acernese, K. Ackley, C. Adams, T. Adams, P. Addesso, R. X. Adhikari *et al.*, Effects of waveform model systematics on the interpretation of GW150914, Classical Quantum Gravity **34**, 104002 (2017).

[29] M. Maggiore, *Gravitational Waves. Vol. 1: Theory and Experiments*, Oxford Master Series in Physics (Oxford University Press, New York, 2007).

[30] V. Cardoso, C. F. B. Macedo, P. Pani, and V. Ferrari, Black holes and gravitational waves in models of minicharged dark matter, J. Cosmol. Astropart. Phys. 5 (2016) 054.

[31] Ø. Christiansen, J. Beltrán Jiménez, and D. F. Mota, Charged black hole mergers: Orbit circularisation and chirp mass bias, arXiv:2003.11452.

[32] L. Liu, Z.-K. Guo, R.-G. Cai, and S. P. Kim, Merger rate distribution of primordial black hole binaries with electric charges, Phys. Rev. D **102**, 043508 (2020).

[33] V. Cardoso, C. F. B. Macedo, P. Pani, and V. Ferrari, Erratum: Black holes and gravitational waves in models of minicharged dark matter, J. Cosmol. Astropart. Phys. 2020 (2020) 01(E).

[34] L. Liu, Ø. Christiansen, Z.-K. Guo, R.-G. Cai, and S. P. Kim, Gravitational and electromagnetic radiation from binary black holes with electric and magnetic charges: Circular orbits on a cone, Phys. Rev. D **102**, 103520 (2020).

[35] H.-T. Wang, P.-C. Li, J.-L. Jiang, Y.-M. Hu, and Y.-Z. Fan, Post-Newtonian waveform for charged binary black hole inspirals and analysis with GWTC-1 events, arXiv: 2004.12421.

[36] B. P. Abbott, R. Abbott, T. D. Abbott, S. Abraham, F. Acernese, K. Ackley, C. Adams, R. X. Adhikari, V. B. Adya, C. Affeldt *et al.*, GWTC-1: A Gravitational-Wave Transient Catalog of Compact Binary Mergers Observed by LIGO and Virgo during the First and Second Observing Runs, Phys. Rev. X **9**, 031040 (2019).

[37] E. Barausse, N. Yunes, and K. Chamberlain, Theory-Agnostic Constraints on Black-Hole Dipole Radiation with Multiband Gravitational-Wave Astrophysics, Phys. Rev. Lett. **116**, 241104 (2016).

[38] N. Yunes, K. Yagi, and F. Pretorius, Theoretical physics implications of the binary black-hole mergers GW150914 and GW151226, Phys. Rev. D **94**, 084002 (2016).

[39] R. L. Arnowitt, S. Deser, and C. W. Misner, The dynamics of general relativity, Gen. Relativ. Gravit. **40**, 1997 (2008).

[40] J. L. Feng, M. Kaplinghat, H. Tu, and H.-B. Yu, Hidden charged dark matter, J. Cosmol. Astropart. Phys. 07 (2009) 004.

[41] L. Ackerman, M. R. Buckley, S. M. Carroll, and M. Kamionkowski, Dark matter and dark radiation, Phys. Rev. D **79**, 023519 (2009).

[42] R. Foot and S. Vagnozzi, Dissipative hidden sector dark matter, Phys. Rev. D **91**, 023512 (2015).

[43] R. Foot and S. Vagnozzi, Diurnal modulation signal from dissipative hidden sector dark matter, Phys. Lett. B **748**, 61 (2015).

[44] R. Foot and S. Vagnozzi, Solving the small-scale structure puzzles with dissipative dark matter, J. Cosmol. Astropart. Phys. 07 (2016) 013.

[45] P. Agrawal, F.-Y. Cyr-Racine, L. Randall, and J. Scholtz, Make dark matter charged again, J. Cosmol. Astropart. Phys. 05 (2017) 022.

[46] S. Davidson, B. Campbell, and D. Bailey, Limits on particles of small electric charge, Phys. Rev. D **43**, 2314 (1991).

[47] M. L. Perl and E. R. Lee, The search for elementary particles with fractional electric charge and the philosophy of speculative experiments, Am. J. Phys. **65**, 698 (1997).

[48] S. Davidson, S. Hannestad, and G. Raffelt, Updated bounds on milli-charged particles, J. High Energy Phys. 5 (2000) 003.

[49] S. L. Dubovsky, D. S. Gorbunov, and G. I. Rubtsov, Narrowing the window for millicharged particles by CMB anisotropy, Sov. J. Exp. Theor. Phys. Lett. **79**, 1 (2004).

[50] A. D. Dolgov, S. L. Dubovsky, G. I. Rubtsov, and I. I. Tkachev, Constraints on millicharged particles from Planck data, Phys. Rev. D **88**, 117701 (2013).

[51] H. Vogel and J. Redondo, Dark radiation constraints on minicharged particles in models with a hidden photon, J. Cosmol. Astropart. Phys. 02 (2014) 029.

[52] P. Gautham A. and S. Sethi, Cosmological implications of electromagnetically interacting dark matter: Milli-charged particles and atoms with singly and doubly charged dark matter, J. Cosmol. Astropart. Phys. 2020 (2020) 039.

[53] R. Plestid, V. Takhistov, Y.-D. Tsai, T. Bringmann, A. Kusenko, and M. Pospelov, New constraints on milli-charged particles from cosmic-ray production, Phys. Rev. D **102**, 115032 (2020).

[54] J. D. Jackson, *Classical Electrodynamics* (Wiley, New York, 1975).

[55] J. Preskill, Magnetic Monopoles, Annu. Rev. Nucl. Part. Sci. **34**, 461 (1984).

[56] D. Stojkovic and K. Freese, A black hole solution to the cosmological monopole problem, Phys. Lett. B **606**, 251 (2005).

[57] J. W. Moffat, Scalar–tensor–vector gravity theory, J. Cosmol. Astropart. Phys. 03 (2006) 004.

[58] J. W. Moffat, Scalar and vector field constraints, deflection of light and lensing in modified gravity (MOG), arXiv:1410.2464.

[59] J. R. Brownstein and J. W. Moffat, Galaxy rotation curves without nonbaryonic dark matter, Astrophys. J. **636**, 721 (2006).

[60] J. R. Brownstein and J. W. Moffat, Galaxy cluster masses without non-baryonic dark matter, Mon. Not. R. Astron. Soc. **367**, 527 (2006).

[61] F. G. Lopez Armengol and G. E. Romero, Scalar-tensor-vector gravity: Solutions with matter content, Boletin de la Asociacion Argentina de Astronomia La Plata Argentina **58**, 231 (2016).

[62] F. G. Lopez Armengol and G. E. Romero, Neutron stars in scalar-tensor-vector gravity, Gen. Relativ. Gravit. **49**, 27 (2017).

[63] F. G. Lopez Armengol and G. E. Romero, Effects of scalar-tensor-vector gravity on relativistic jets, Astrophys. Space Sci. **362**, 214 (2017).

[64] F. Shojai, S. Cheraghchi, and H. Bouzari Nezhad, On the gravitational instability in the Newtonian limit of MOG, Phys. Lett. B **770**, 43 (2017).

[65] D. Pérez, Federico G. Lopez Armengol, and G. E. Romero, Accretion disks around black holes in scalar-tensor-vector gravity, Phys. Rev. D **95**, 104047 (2017).

[66] N. Ghafourian and M. Roshan, Global stability of self-gravitating discs in modified gravity, Mon. Not. R. Astron. Soc. **468**, 4450 (2017).

[67] M. A. Green, J. W. Moffat, and V. T. Toth, Modified gravity (MOG), the speed of gravitational radiation and the event GW170817/GRB170817A, Phys. Lett. B **780**, 300 (2018).

[68] J. W. Moffat, LIGO GW150914 and GW151226 gravitational wave detection and generalized gravitation theory (MOG), Phys. Lett. B **763**, 427 (2016).

[69] F. Löffler, J. Faber, E. Bentivegna, T. Bode, P. Diener, R. Haas, I. Hinder, B. C. Mundim, C. D. Ott, E. Schnetter, G. Allen, M. Campanelli, and P. Laguna, The Einstein toolkit: A community computational infrastructure for relativistic astrophysics, Classical Quantum Gravity **29**, 115001 (2012).

[70] Collaborative Effort, Einstein Toolkit for Relativistic Astrophysics, Astrophysics Source Code Library (2011), https://doi.org/10.5281/zenodo.4298887.

[71] M. Babiuc-Hamilton *et al.*, The Einstein toolkit (2019), to find out more, visit http://einsteintoolkit.org.

[72] K. S. Thorne and D. MacDonald, Electrodynamics in curved spacetime $-3+1$ formulation, Mon. Not. R. Astron. Soc. **198**, 339 (1982).

[73] M. Alcubierre, Introduction to $3+1$ Numerical Relativity (Oxford University Press, Oxford, UK, 2008).

[74] T. W. Baumgarte and S. L. Shapiro, *Numerical Relativity: Solving Einstein's Equations on the Computer* (Cambridge University Press, Cambridge, England, 2010).

[75] M. Shibata, *Numerical Relativity* (World Scientific Publishing Co, Singapore, 2016).

[76] See Supplemental Material at http://link.aps.org/supplemental/10.1103/PhysRevLett.126.041103 for details on the numerical methods, convergence properties, and a discussion on confidence levels.

[77] M. Zilhão, V. Cardoso, C. Herdeiro, L. Lehner, and U. Sperhake, Collisions of charged black holes, Phys. Rev. D **85**, 124062 (2012).

[78] M. Zilhão, V. Cardoso, C. Herdeiro, L. Lehner, and U. Sperhake, Collisions of oppositely charged black holes, Phys. Rev. D **89**, 044008 (2014).

[79] G. Bozzola and V. Paschalidis, Initial data for general relativistic simulations of multiple electrically charged black holes with linear and angular momenta, Phys. Rev. D **99**, 104044 (2019).

[80] J. M. Bowen and J. W. York, Time asymmetric initial data for black holes and black hole collisions, Phys. Rev. D **21**, 2047 (1980).

[81] J. M. Bowen, Inversion symmetric initial data for *N* charged black holes, Ann. Phys. (N.Y.) **165**, 17 (1985).

[82] M. Alcubierre, J. C. Degollado, and M. Salgado, Einstein-Maxwell system in $3 + 1$ form and initial data for multiple charged black holes, Phys. Rev. D **80**, 104022 (2009).

[83] H. Witek and M. Zilhão, CANUDA code (2015), https://bitbucket.org/canuda/.

[84] H. Witek, M. Zilhao, G. Ficarra, and M. Elley, CANUDA: A public numerical relativity library to probe fundamental physics (2020), https://doi.org/10.5281/zenodo.3565475.

[85] U. Sperhake, Binary black-hole evolutions of excision and puncture data, Phys. Rev. D **76**, 104015 (2007).

[86] M. Zilhão, H. Witek, and V. Cardoso, Nonlinear interactions between black holes and Proca fields, Classical Quantum Gravity **32**, 234003 (2015).

[87] M. Shibata and T. Nakamura, Evolution of three-dimensional gravitational waves: Harmonic slicing case, Phys. Rev. D **52**, 5428 (1995).

[88] T. W. Baumgarte and S. L. Shapiro, Numerical integration of Einstein's field equations, Phys. Rev. D **59**, 024007 (1998).

[89] E. Schnetter, S. H. Hawley, and I. Hawke, Evolutions in 3-D numerical relativity using fixed mesh refinement, Classical Quantum Gravity **21**, 1465 (2004).

[90] E. Newman and R. Penrose, An approach to gravitational radiation by a method of spin coefficients, J. Math. Phys. (N.Y.) **3**, 566 (1962).

[91] C. Reisswig and D. Pollney, Notes on the integration of numerical relativity waveforms, Classical Quantum Gravity **28**, 195015 (2011).

[92] B. P. Abbott, R. Abbott, T. D. Abbott, M. R. Abernathy, F. Acernese, K. Ackley, C. Adams, T. Adams, P. Addesso, R. X. Adhikari *et al.*, Properties of the Binary Black Hole Merger GW150914, Phys. Rev. Lett. **116**, 241102 (2016).

[93] T. Damour, B. R. Iyer, and B. S. Sathyaprakash, Improved filters for gravitational waves from inspiraling compact binaries, Phys. Rev. D **57**, 885 (1998).

[94] N. Aghanim *et al.* (Planck Collaboration), Planck 2018 results. VI. Cosmological parameters, Astron. Astrophys. **641**, A6 (2020).

[95] LIGO Scientific Collaboration, Advanced LIGO anticipated sensitivity curves (2009), https://dcc.ligo.org/LIGO-T0900288/public.

[96] B. P. Abbott, R. Abbott, T. D. Abbott, M. R. Abernathy, F. Acernese, K. Ackley, C. Adams, T. Adams, P. Addesso, R. X. Adhikari *et al.*, Tests of General Relativity with GW150914, Phys. Rev. Lett. **116**, 221101 (2016).

[97] P. Jai-akson, A. Chatrabhuti, O. Evnin, and L. Lehner, Black hole merger estimates in Einstein-Maxwell and Einstein-Maxwell-dilaton gravity, Phys. Rev. D **96**, 044031 (2017).

[98] J. W. Moffat, Black holes in modified gravity (MOG), Eur. Phys. J. C **75**, 175 (2015).

[99] V. Varma, S. E. Field, M. A. Scheel, J. Blackman, L. E. Kidder, and H. P. Pfeiffer, Surrogate model of hybridized numerical relativity binary black hole waveforms, Phys. Rev. D **99**, 064045 (2019).